

The superconducting state of  $\text{Sr}_x\text{Mo}_6\text{S}_8$  ( $x \leq 1.0$ ) by simultaneous application of chemical and external pressure

This article has been downloaded from IOPscience. Please scroll down to see the full text article.

1991 J. Phys.: Condens. Matter 3 2471

(<http://iopscience.iop.org/0953-8984/3/15/002>)

View [the table of contents for this issue](#), or go to the [journal homepage](#) for more

Download details:

IP Address: 171.66.16.151

The article was downloaded on 11/05/2010 at 07:11

Please note that [terms and conditions apply](#).

## The superconducting state of $\text{Sr}_x\text{Mo}_6\text{S}_8$ ( $x \leq 1.0$ ) by simultaneous application of chemical and external pressure

J Beille†, H Schmitt‡, O Peña‡, J Padiou‡ and M Sergent‡

† Laboratoire Louis Néel, CNRS 38042 Grenoble Cédex, France

‡ Laboratoire de Chimie Minérale B, URA CNRS 254, Université de Rennes I, 35042 Rennes Cédex, France

Received 11 October 1990

**Abstract.** Single crystals of  $\text{Sr}_x\text{Mo}_6\text{S}_8$  with different strontium concentrations ( $x \leq 1.0$ ) have been grown, and their transport properties studied under zero and applied pressure. The structural transition from a high-temperature rhombohedral symmetry towards a low-temperature triclinic structure is strongly sample dependent, and is clearly inhibited by the ‘chemical pressure’ set up by the strontium vacancies in the lattice. However, this effect is not strong enough to completely suppress the structural transition, and further application of an external pressure is necessary to attain the superconducting state ( $T_c > 10$  K under 20 kbar). The structural transition ( $T_s$ ) and superconducting critical ( $T_c$ ) temperatures under pressure for stoichiometric and substoichiometric samples can be described by the same curve, if chemical pressure is taken into account. Comparison is made with  $\text{EuMo}_6\text{S}_8$  and related compounds where the cations are magnetic.

### 1. Introduction

The divalent-cation Chevrel phase compounds  $\text{EuMo}_6\text{S}_8$ ,  $\text{BaMo}_6\text{S}_8$ ,  $\text{SrMo}_6\text{S}_8$  and  $\text{CaMo}_6\text{S}_8$ , undergo a structural transition at  $T = T_s$  [1–3], leading to partial localization of the conduction electrons, which could explain the absence of superconductivity in these compounds. Under pressure, the crystallographic transformation is inhibited, and the metallic high-temperature hexagonal–rhombohedral symmetry may be preserved. The appearance of superconductivity under pressure was first made evident above 7 kbar in  $\text{EuMo}_6\text{S}_8$  [4–6]. Superconductivity was later achieved above about 20 kbar in  $\text{BaMo}_6\text{S}_8$  [7].  $\text{CaMo}_6\text{S}_8$  seems to be a limiting case in the series as the effect of Ca defects results in a ‘chemical pressure’ on the calcium site, which by itself induces a superconducting transition at about 9.5 K [8, 9].

In this paper, we report the occurrence of superconductivity in single crystals of  $\text{SrMo}_6\text{S}_8$  as well as in cation deficient  $\text{Sr}_x\text{Mo}_6\text{S}_8$  ( $x < 1$ ) under high pressures above about 20 kbar.

### 2. Experiment

Single crystals were grown from a melt composed basically of mechanical mixtures of  $\text{SrMo}_6\text{S}_8$  and SrS. Pellets of the starting mixtures were placed in alumina containers

inside outgassed molybdenum crucibles. No sealing of the crucibles was performed, and the ensemble was heated in a high-temperature graphite-resistor furnace under a continuous flow of high purity argon. Melting was achieved at about 1845 °C, immediately followed by cooling: first rapid ( $\approx 100$  °C/h) down to 1840 °C, then slower ( $-30$  °C/h down to 1830 °C, next  $-200$  °C/h down to 1500 °C) and finally on the furnace thermal inertia. By this procedure, the destruction process of mainly the liquid phase can be delayed by additional melting of solid state material in equilibrium with the melt, and thus the slope of the liquid–solid equilibrium surface followed during the process of crystallization [10].

In order to study the vacancy dependence of the physical properties, two starting compositions were selected: (i)  $\text{SrMo}_6\text{S}_8 + \text{SrS}$  ( $\text{Sr}_{0.118}\text{Mo}_{0.353}\text{S}_{0.529}$ ); (ii)  $\text{Sr}_{0.815}\text{Mo}_6\text{S}_8$  ( $\text{Sr}_{0.055}\text{Mo}_{0.405}\text{S}_{0.54}$ ). In (i), the excess strontium sulphide ensures full stoichiometric conditions (1 : 6 : 8) of the single crystals, since the cation concentration cannot be larger than unity [11]. On the other hand, when the starting mixture is too close to the ideal Chevrel phase stoichiometry, the compositional shifts occurring during the crystal growth [10, 12] would undoubtedly lead to strontium deficiencies, more or less pronounced depending on the cooling conditions. In this way, two different sets of crystals—hereafter called stoichiometric (composition (i)) and substoichiometric (composition (ii))—were obtained, from which we have chosen the main specimens studied in this work.

Resistivity measurements under hydrostatic pressure were performed using a beryllium–copper self-clamping cell to pressurize, inside a teflon capsule, a lead manometer and the sample by means of a 1 : 1 mixture of isoamyl alcohol and *n*-pentane. Pressures were derived from the superconducting transition of a lead manometer. Contacts were indium soldered on the samples with an ultrasonic wire. AC resistivity measurements were performed in a helium flow cryostat using a lock-in amplifier.

### 3. Results

#### 3.1. Structural refinement

Two small single crystals were selected from the stoichiometric and substoichiometric preparations, respectively, and their crystal structure refined at room temperature following the methods described elsewhere [11, 12]. Their structure can be described in the same way as the other large cation based chevrel phase materials with, in particular, along a three-fold axis, the stacking of two  $\text{Mo}_6\text{S}_8$  units and a  $\text{SrS}_8$  pseudo-cubic site of a hexagonal–rhombohedral unit cell [11]. Particular attention was paid to the occupancy of the origin site by the strontium cation: stoichiometric material did indeed contain 0.995 (3) Sr atoms per mole, confirming that occupancy did not exceed unity in spite of the excess strontium in the starting mixture. Refinement of the substoichiometric crystal resulted in a strontium occupancy of 0.952 (2), that is, strontium vacancies at the origin site. No other sites were occupied by the strontium atoms, as verified by a final difference map of the electron densities. Reliability factors  $R$  and  $R_w$  were better than (2.1%) and (3.2%), respectively.

The principal interatomic distances describing the structure are summarized in table 1. The  $(\text{Mo}–\text{Mo})^{\text{intra}}$  distances are specially interesting since they characterize the size of the  $\text{Mo}_6$  cluster. The intercluster  $(\text{Mo}–\text{Mo})^{\text{inter}}$  distance follows the same evolution as the lattice parameters of the rhombohedral lattice [11]. The Sr–S(1) and the Sr–S(2)

**Table 1.** Lattice parameters and main interatomic distances (in Å) for  $Sr_xMo_6S_8$  ( $x = 1.0$  and  $0.95$ ). Space group  $R\bar{3}$ ;  $Z = 1$ . The estimated standard deviations are given in parentheses. (Mo–Mo) $\Delta^{intra}$  concerns atoms belonging to the same  $Mo_6$  cluster and situated on the same plane perpendicular to the ternary axis; (Mo $\Delta$ –Mo $\Delta$ ) $^{intra}$  concerns atoms belonging to the same  $Mo_6$  cluster, but situated on two neighbouring planes.

	$SrMo_6S_8$	$Sr_{0.95}Mo_6S_8$
$a_R$ (Å)	6.5732 (6)	6.5674 (6)
$\alpha_R$ (°)	88.98 (1)	89.02 (3)
$V_R$ (Å <sup>3</sup> )	283.88 (9)	283.1 (1)
<b><math>Mo_6S_8</math> cube</b>		
(Mo–Mo) $\Delta^{intra}$	$2 \times 2.6663$ (3)	$2 \times 2.6680$ (4)
(Mo $\Delta$ –Mo $\Delta$ ) $^{intra}$	$2 \times 2.7137$ (3)	$2 \times 2.7155$ (4)
(Mo–Mo) $^{inter}$	3.3012 (4)	3.2942 (4)
(Mo–S(1)) $^{intra}$	2.4531 (6)	2.4510 (7)
	2.4637 (6)	2.4601 (7)
	2.5070 (6)	2.5068 (7)
(Mo–S(1)) $^{inter}$	2.5892 (6)	2.5860 (7)
Mo–S(2)	2.3901 (6)	2.3909 (4)
<b><math>SrS_8</math> cube</b>		
Sr–S(1)	3.1262 (6)	3.1234 (7)
Sr–S(2)	2.8469 (6)	2.8371 (4)

distances describe the size of the pseudo-cubic  $SrS_8$  origin site. Our results show that, with increasing cationic vacancies (from  $x = 1.0$  to  $x = 0.95$ ), a slight expansion of the metallic  $Mo_6$  cluster occurs, due to a weakening of the metal–metal bonds. At the same time, a decrease of the lattice volume  $V_R$  is observed. These two opposite variations lead to a contraction of the origin site, resulting in an internal ('chemical') pressure which would partly inhibit the structural transformation (rhombohedral  $\rightarrow$  triclinic) at low temperature.

### 3.2. Resistivity under pressure

Single crystals of well defined shape were chosen from the stoichiometric and substoichiometric preparations. The former,  $SrMo_6S_8$  (SMS), is about  $0.14 \times 0.42 \times 0.7$  mm<sup>3</sup>. The substoichiometric crystal, grown from a starting mixture  $Sr_{0.815}Mo_6S_8$  ( $S_xMS$ ), is about  $0.1 \times 0.14 \times 0.65$  mm<sup>3</sup>. The exact composition of the substoichiometric single crystal was, however, not exactly defined as no microprobe analysis had been performed up to this point [13].

The resistivity of both samples is about  $500 \mu\Omega$  cm at room temperature. In figures 1 and 2 we give the resistivity curves obtained at normal pressure as well as under pressures of up to 20 kbar. We observed a discontinuity in the resistivity which is associated with the structural transformation (rhombohedral  $\rightarrow$  triclinic) which has been made evident earlier by specific heat experiments [2]. At normal pressure, the resistivity transition is very sharp for the stoichiometric sample and more spread (over a range of  $\approx 6$  K) for the substoichiometric one. We find  $T_S \approx 134.4$  K for the former and  $T_S \approx 128.2$  K for the latter one at ambient pressure, which can be compared with

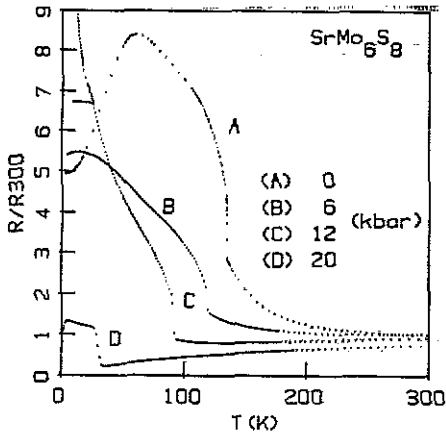


Figure 1. Temperature dependence of the normalized resistivity of a  $\text{SrMo}_6\text{S}_8$  single crystal under various pressures.

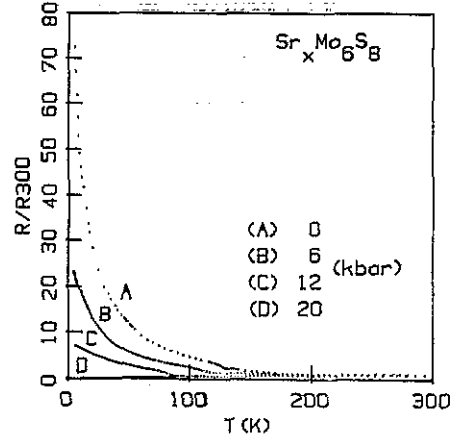


Figure 2. Temperature dependence of the normalized resistivity of a  $\text{Sr}_x\text{Mo}_6\text{S}_8$  single crystal under various pressures.

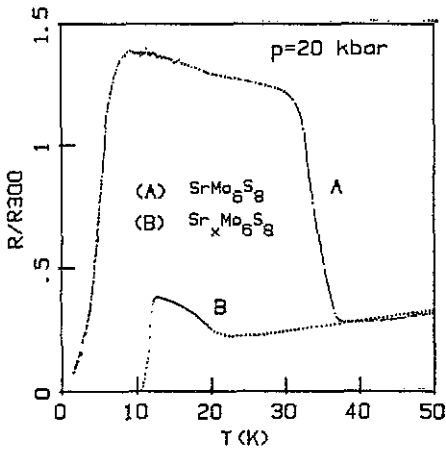


Figure 3. Temperature dependence of the normalized resistivity of (A)  $\text{SrMo}_6\text{S}_8$  and (B)  $\text{Sr}_x\text{Mo}_6\text{S}_8$  under 20 kbar.

$T_s \approx 139$  K for sintered samples from specific heat experiments. Between room temperature and  $T_s$  the resistivity increases at decreasing temperature. Below  $T_s$  the resistivity behaviour of the two samples differs: in SMS the resistivity passes through a maximum around 60 K before decreasing in a  $T^2$  metallic-like dependence whereas in  $\text{S}_x\text{MS}$  the resistivity increases at decreasing temperature in a semiconducting-like behaviour till the lowest measuring temperature of 1.5 K.

Under various increasing pressures, the resistivity at 1.5 K and the structural transition temperature ( $T_s$ ) of  $\text{S}_x\text{MS}$  decrease simultaneously, and superconductivity appears at below 20 kbar, as illustrated in figure 3. A similar trend is observed above a pressure threshold of  $\approx 12$  kbar for SMS. For this latter sample, between the normal pressure and 12 kbar, the low temperature dependence of resistivity changes from a behaviour with a maximum to a monotonic semiconducting-like behaviour similar to that of  $\text{S}_x\text{MS}$ . Under 20 kbar, the structural transition coexists with the superconducting state for both

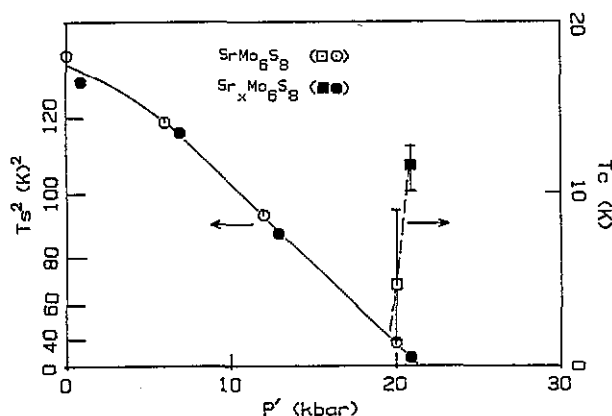


Figure 4. Dependence of  $T_S^2$  and  $T_c^*$  as a function of the effective pressure  $p'$  (see text) for  $SrMo_6S_8$  and  $Sr_xMo_6S_8$ . The bars are the onset and the zero-resistance temperature widths.

compounds (table 2). Above 20 kbar  $Sr_xMo_6S_8$  has, as a minimum, the same  $T_c$  value as that of  $EuMo_6S_8$  under  $\sim 12.7$  kbar (maximum of  $T_c$ ) [14].

Enlargement of the low temperature parts of the resistivity curves of both samples under 20 kbar is given in figure 3. At a given pressure,  $T_S$  is lower for  $s_xMS$  than for SMS, which can be interpreted in terms of an internal chemical pressure in the sub-stoichiometric sample as the lattice parameter decreases when vacancy concentration increases (table 1), in a similar manner to the case of  $Ca_xMo_6S_8$  compounds [8, 9].

Plots of  $T_S$  as a function of the pressure for both single crystals fall on the same curve if the pressures applied on  $s_xMS$  are increased by the same value of  $\approx 0.90$  kbar, which we take to be the internal chemical pressure ( $p_i$ ). In figure 4, we have plotted  $T_S^2$  and  $T_c$  as a function of an effective pressure ( $p'$ ) which is the external pressure  $p$  for SMS and  $p + p_i$  for  $s_xMS$ . Plots of  $T_S^2(p')$  lie on a straight line over a large range of pressure (for  $T_S \leq 120$  K) and extrapolate to zero for a critical pressure  $p'_c \approx 21.4$  kbar. Such a relation  $T_S^2 \propto (p' - p'_c)$  was also found for  $EuMo_6S_8$  [6].

#### 4. Discussion

The present experimental results on  $SrMo_6S_8$  and  $Sr_xMo_6S_8$  show strong similarities with those observed in  $EuMo_6S_8$ . We found a semimetal- or metal-like behaviour depending on the stoichiometry of the samples and on the pressure range. Analogously,

Table 2. Structural transition temperature ( $T_S$ ), superconducting onset ( $T_{c,on}$ ) and midpoint ( $T_{c,mid}$ ) resistive transition temperature of  $Sr_xMo_6S_8$  ( $x = 1.0$  and  $0.95$ ).

	$SrMo_6S_8$	$Sr_{0.95}Mo_6S_8$
$T_S$ (K)	36.6	21.9
$T_{c,on}$ (K)	9	12.7
$T_{c,mid}$ (K)	4.7	11.6

single crystals of  $\text{EuMo}_6\text{S}_8$  are very sensitive to defects or stoichiometry as has been made evident in samples presenting a semimetal-like behaviour [15] or metal-like one [16, 17]. Under pressure the behaviour of the Sr-based compounds is also very similar to that of  $\text{EuMo}_6\text{S}_8$ . The structural transition temperature ( $T_S$ ) decreases under pressure and above a threshold of pressure; a correlation is observed between the decrease of  $T_S$ , the increase of the carriers number at low temperature (as deduced from resistivity and leading to the appearance of superconductivity), and the initial increase of the critical temperature ( $T_C$ ). Such correlations have also been found as a function of internal chemical pressure produced by cation substitution in  $\text{Eu}_{1-x}\text{Yb}_x\text{Mo}_6\text{S}_8$  [18],  $\text{Eu}_{1-x}\text{Sn}_x\text{Mo}_6\text{S}_8$  [5] and in  $\text{Ca}_x\text{Mo}_6\text{S}_8$  [8, 9]. This type of behaviour under chemical or external pressure seems to be general for the case of divalent-cation Chevrel phases.

The structural transition in  $\text{EuMo}_6\text{S}_8$  and  $\text{BaMo}_6\text{S}_8$  was ascribed to a Jahn-Teller-like electronic instability arising from the triclinic distortion of the  $\text{Mo}_6$  octahedra, and leading to a partial localization of the conduction electrons [2]. Such mechanisms may be extended to  $\text{SrMo}_6\text{S}_8$ , as shown by the single-crystal x-ray data of table 1. Under hydrostatic pressure such deformation is prevented, although charge transfer effects remain unchanged.

Some authors directly relate the appearance of superconductivity under pressure to the decrease of the number of states localized at the structural transition [19], a proposition that is supported by the correlations observed. An alternative hypothesis, based on the existence of a maximum and a  $T^2$  decrease in the resistivity of a  $\text{EuMo}_6\text{S}_8$  single crystal, is the existence of Mo spin fluctuations inhibiting superconductivity. Pressure could increase the spin fluctuation temperature, thus leading to the appearance of superconductivity [16, 17]. However, in the assumption that a common behaviour can be established for the divalent-cation Chevrel phase, the evolution from a decreasing  $T^2$ -like resistivity curve to a semimetallic one under pressure in  $\text{SrMo}_6\text{S}_8$  seems to conflict with this last hypothesis.

A principal interest of studying such compounds is the possibility of making comparisons with  $\text{EuMo}_6\text{S}_8$ , in which several properties depend on the magnetic state of the cation. In particular,

(i) a smaller effect of the magnetic field on the low temperature resistivity is expected if the semimetal model of two weakly overlapping bands is verified [20],

(ii) the comparison of the upper critical fields of  $\text{SrMo}_6\text{S}_8$  and  $\text{EuMo}_6\text{S}_8$  can allow verification of the existence of a negative exchange field due to the presence of a rare-earth in the latter [21].

With this in mind, magnetoresistance measurements performed under pressure on  $\text{SrMo}_6\text{S}_8$  and  $\text{Sr}_x\text{Mo}_6\text{S}_8$  single crystals are now in progress.

## References

- [1] Baillif R, Junod A, Lachal B, Muller J and Yvon K 1981 *Solid State Commun.* **40** 603
- [2] Baillif R, Dunand A, Muller J and Yvon K 1981 *Phys. Rev. Lett.* **47** 672
- [3] Lachal B, Baillif R, Junod A and Muller J 1983 *Solid State Commun.* **45** 849
- [4] Chu C W, Huang S Z, Lin C H, Meng R L, Wu M K and Schmidt P H 1981 *Phys. Rev. Lett.* **46** 276
- [5] Harrison D W, Lim K C, Thompson J D, Huang C Y, Hambourger P D and Luo H L 1981 *Phys. Rev. Lett.* **46** 280
- [6] Decroux M, Torikachvili M S, Maple M B, Baillif R, Fischer Ø and Muller J 1983 *Phys. Rev. B* **28** 6270
- [7] Yao Y S, Guertin R P, Hinks D G, Jorgensen J and Capone D W 1988 *Phys. Rev. B* **37** 5032

- [8] Geantet C, Padiou J, Peña O, Sergent M and Horyn R 1987 *Solid State Commun.* **64** 1363
- [9] Geantet C, Horyn R, Padiou J, Peña O and Sergent M 1988 *Physica C* **153-5** 481
- [10] Horyn R, Peña O, Geantet C and Sergent M 1989 *Supercond. Sci. Technol.* **2** 71
- [11] Peña O and Sergent M 1989 *Prog. Solid State Chem.* **19** 165
- [12] Peña O, Horyn R, Potel M, Padiou J and Sergent M 1985 *J. Less-Common Met.* **105** 105
- [13] Exact composition, as determined from wds microprobe analysis, will be given in a forthcoming work
- [14] Cheaito B 1986 *PhD Thesis* Grenoble University
- [15] Peña O, Horyn R, Geantet C, Gougeon P, Padiou J and Sergent M 1986 *J. Solid State Chem.* **63** 62
- [16] Holtzberg F, Flouquet J, Konczykowski M, Sulpice A and Tournier R 1985 *J. Appl. Phys.* **57** 3067
- [17] Konczykowski M, Holtzberg F, Horn P, Laplaca S, Sulpice A and Tournier R 1986 *J. Magn. Magn. Mat.* **54-7** 1523
- [18] Beille J, Cheaito B, Maple M B and Torikachvili M 1984 *Ann. Chim., Fr.* **9** 1007
- [19] Lacroix R C, Wolf S A, Chaikin P M, Huang C Y and Luo H L 1982 *Phys. Rev. Lett.* **48** 1212
- [20] Meul H W, Decroux M, Odermatt R, Noer R and Fischer Ø 1982 *Phys. Rev. B* **26** 6431
- [21] Decroux M and Fischer Ø 1982 *Superconductivity in Ternary Compounds II* ed M B Maple and Ø Fischer (Berlin: Springer) p 58